J Sci Comput
DOI 10.1007/s10915-016-0264-z

Direct Discontinuous Galerkin Method and Its Variations for Second Order Elliptic Equations

Hongying Huang[1,2] · **Zheng Chen**[3] · **Jin Li**[4] · **Jue Yan**[3]

Received: 15 December 2015 / Revised: 10 June 2016 / Accepted: 9 August 2016

Abstract In this paper, we study direct discontinuous Galerkin method (Liu and Yan in SIAM J Numer Anal 47(1):475–698, 2009) and its variations (Liu and Yan in Commun Comput Phys 8(3):541–564, 2010; Vidden and Yan in J Comput Math 31(6):638–662, 2013; Yan in J Sci Comput 54(2–3):663–683, 2013) for 2nd order elliptic problems. A priori error estimate under energy norm is established for all four methods. Optimal error estimate under L^2 norm is obtained for DDG method with interface correction (Liu and Yan in Commun Comput Phys 8(3):541–564, 2010) and symmetric DDG method (Vidden and Yan in J Comput Math 31(6):638–662, 2013). A series of numerical examples are carried out to illustrate the accuracy and capability of the schemes. Numerically we obtain optimal $(k+1)$th order convergence for DDG method with interface correction and symmetric DDG method on nonuniform and unstructured triangular meshes. An interface problem with discontinuous diffusion coefficients is investigated and optimal $(k+1)$th order accuracy is obtained. Peak solutions with sharp transitions are captured well. Highly oscillatory wave solutions of Helmholz equation are well resolved.

✉ Jue Yan
jyan@iastate.edu

Hongying Huang
huanghy@lsec.cc.ac.cn

Zheng Chen
zchen@iastate.edu

Jin Li
lijin@lsec.cc.ac.cn

1 School of Mathematics, Physics and Information Science, Zhejiang Ocean University, Zhoushan, Zhejiang, China

2 Key Laboratory of Oceanographic Big Data Mining and Application of Zhejiang Province, Zhoushan, Zhejiang, China

3 Department of Mathematics, Iowa State University, Ames, IA 50011, USA

4 School of Science, Shandong Jianzhu University, Jinan, Shandong, China

Published online: 23 August 2016

Keywords Discontinuous Galerkin method · Second order elliptic problem

1 Introduction

In this article, we consider to study direct discontinuous Galerkin finite element method [17] and its variations [18,24,27] for 2nd order elliptic problem,

$$-\nabla \cdot (K(\mathbf{x})\nabla u) + c(\mathbf{x})u = f, \quad \text{in } \Omega \subset \mathbb{R}^2, \tag{1.1}$$

associated with Dirichlet boundary condition $u = u_0$ on $\partial\Omega$. To simplify the presentation, we focus on model problem (1.1) under two-dimensional setting. We have $\mathbf{x} = (x_1, x_2) \in \Omega$ with Ω as a bounded and simply connected polygonal domain. Diffusion coefficient matrix is denoted as $K(\mathbf{x})$ and is assumed being uniformly positive definite. Here f is a given function in $L^2(\Omega)$. We assume the data in Eq. (1.1) satisfy standard regularity assumptions. The special case of (1.1) is the Poisson's equation,

$$-\triangle u = f, \tag{1.2}$$

and Laplace's equation of (1.2) with $f = 0$.

In literature we have enormous amount of articles discuss numerical methods solving problem (1.1). We skip the long review list. Singular solutions may arise from elliptic problem (1.1) on none smooth domains, with combined boundary conditions or discontinuous diffusion coefficients. These singularities impose challenges and various difficulties on the development of accurate and efficient numerical methods solving (1.1). In this paper, we study direct discontinuous Galerkin finite element method [17] and its variations [18,24,27] on the model problem (1.1). Discontinuous Galerkin (DG) method is a class of finite element method that use completely discontinuous piecewise functions as the numerical approximations. Basis functions are completely discontinuous across element edges, thus DG methods have the flexibility that is not shared by standard finite element methods, such as the allowance of arbitrary triangulations with hanging nodes, complete freedom of choosing polynomial degrees in each element (p-adaptivity), and extremely local data structure. It is believed that DG method is especially suitable to capture solutions with sharp transitions or discontinuities, and solutions with complex structures. We refer to review articles [10,12,23] for the successful developments of DG methods on convection diffusion problems and refer to recent books [13,16,21] on DG methods.

There are several DG methods for solving elliptic and parabolic problems. One class is the *interior penalty* (IP) methods, dates back to 1982 by Arnold in [1] (also by Baker in [3] and Wheeler in [26]), the Baumann and Oden [5,19] and NIPG [22] methods. Another class is closely related to mixed finite element methods [8,20], the *local discontinuous Galerkin* method introduced in [11] by Cockburn and Shu (originally studied by Bassi and Rebay in [4] for compressible Navier–Stokes equations). We refer to the unified analysis paper [2] in 2002 for the review of different diffusion DG solvers. Recent developments of DG methods on elliptic problems include the over penalized DG method [6], the hybridized DG method [9] and the weak Galerkin method [25], etc.

In [17] we developed a direct discontinuous Galerkin (DDG) method solving time dependent diffusion equations. The key contribution of [17] is the introduction of numerical flux $\widehat{u_x}$ that approximates the solution derivative u_x at the discontinuous element edge. The numerical flux formula $\widehat{u_x}$ designed in [17] involves the solution jump $[\![u]\!]$, solution derivative average $\{\{u_x\}\}$ and higher order derivative jump values of u across element edge. The scheme

is directly based on the weak formulation of the diffusion equation, thus gains its name the direct DG method. Due to accuracy loss with high order approximations, in [18] we further developed DDG method with interface correction. Numerically we obtain optimal $(k+1)$th order convergence in [18] with a small fixed penalty coefficient applied. As is well known, the penalty coefficient of symmetric interior penalty method (SIPG) method depends on the approximation polynomial degree and needs to be large enough to stablize the scheme. We also have the symmetric version [24] and nonsymmetric version [27] of the DDG method. Compared to NIPG method [22], nonsymmetric DDG method [27] obtains optimal order convergence with any degree polynomial approximations.

In this article, we further develop DDG method [17] and its variations [18,24,27] to solve elliptic model problem (1.1). Continuity and coercivity of the primal bilinear form are obtained. A priori error estimate under energy norm is established for all four DDG methods. A priori optimal error estimate under L^2 norm is obtained for DDG method with interface correction [18] and symmetric DDG method [24].

A series of numerical examples are carried out to illustrate the accuracy and capability of the methods. With P_k polynomial approximations we obtain optimal $(k+1)$th order convergence for DDG method with interface correction [18] and symmetric DDG method [24] on nonuniform and unstructured triangular meshes. Then we focus on numerical studies of these two DDG methods. An interface problem with discontinuous diffusion coefficients is investigated and optimal $(k+1)$th order accuracy is obtained even the solution itself is not even $C^1(\Omega)$ across interface lines. For the interface problem we make no modification on scheme formulations and the zero flux jump condition is simply applied weakly through the numerical flux defined on element edges. Peak solution with sharp transitions is captured well with these two DDG methods. Highly oscillatory wave solutions of Helmholz equation are well resolved. Among the four DDG methods, symmetric DDG method [24] is shown to be the most suitable elliptic solver not only because the linear system is symmetric (for Laplace for example) such that faster solvers can be applied. Under same settings the symmetric DDG method resolves the highly oscillatory wave better than the DDG method with interface correction. When comparing to SIPG method [1], symmetric DDG method roughly saves 7–10 % on CPU time with high order and on refined mesh simulations.

The rest of the article is organized as follows. In Sect. 2, we present scheme formulations of DDG method and its variations applied to model problem (1.2) and problem (1.1) with variable coefficient diffusion matrix. In Sect. 3 we present stability and a priori error estimate under a standard energy norm and L^2 norm. Finally numerical examples are shown in Sect. 4.

Throughout this paper, we let $|\cdot|_{H^s(K)}$ and $\|\cdot\|_{H^s(K)}$ denote the seminorm and norm of space $H^s(K)$, $s \geq 0$, respectively. Let $\mathbf{H}^s(K)$ denote the space of $H^s(K) \times H^s(K)$ and $\mathbf{L}^2(K)$ the space of $L^2(K) \times L^2(K)$.

2 Discretization of Direct DG Method and Its Variations

Let $\mathcal{T}_h$ be a shape-regular partition of the domain Ω into disjoint elements $\{K\}_{K\in\mathcal{T}_h}$, for example triangles or quadrilaterals with $\bar{\Omega} = \cup_{K\in\mathcal{T}_h}\bar{K}$. By $h_K = \text{diam}(K)$, we denote the diameter of an element $K \in \mathcal{T}_h$. We set $h = \max_{K\in\mathcal{T}_h} h_K$ as the mesh size of the partition. We denote by $\mathcal{E}_h^I$ the set of all internal edges, and by $\mathcal{E}_h^D$ the set of all boundary edges of $\mathcal{T}_h$. And we have $\mathcal{E}_h = \mathcal{E}_h^I \cup \mathcal{E}_h^D$ as the collection of all edges. The length of the edge $e \in \mathcal{E}_h$ is denoted by h_e.

We have $P_k(K)$ representing the polynomials function space of degree at most k on element K. The DG solution space is defined as,

$$V_h^k := \{v \in L^2(\Omega) : v|_K \in P_k(K), \forall K \in \mathcal{T}_h\}.$$

Suppose K and K' are two adjacent elements and share one common edge e. There are two traces of v along the edge e, where we add or subtract those values to obtain the average and the jump. We denote by $\mathbf{n} = (n_1, n_2)^T$ the outward unit normal vector pointing from K into its neighbor element K'. Now the average and the jump of v over edge e are defined and denoted as follows,

$$\{\{v\}\} = \frac{1}{2}\left(v|_K + v|_{K'}\right), \quad [\![v]\!] = v|_{K'} - v|_K, \quad \forall e = \partial K \cap \partial K'.$$

Let's use Poisson Eq. (1.2) to illustrate Direct DG [17] and its variations [18,24,27] schemes formulations. Multiply Eq. (1.2) with arbitrary smooth test function v, integrate over element $K \in \mathcal{T}_h$, have the integration by parts and we obtain,

$$\int_K \nabla u \cdot \nabla v d\mathbf{x} - \int_{\partial K} \nabla u \cdot \mathbf{n} v ds = \int_K f v d\mathbf{x}. \tag{2.1}$$

The idea of Direct DG method [17] is to design a formula to approximate the gradient ∇u across the discontinuous element edge and obtain a DG method that is based directly on the weak formulation (2.1) of (1.2). *With no ambiguity, for the rest of this article we use same letter u instead of notation u_h to represent DG numerical solution*. Now the Direct DG method of (1.2) is defined as, we seek numerical solution $u \in V_h^k$ such that for all test function $v \in V_h^k$ we have,

$$\int_K \nabla u \cdot \nabla v d\mathbf{x} - \int_{\partial K} \widehat{u_{\mathbf{n}}} v ds = \int_K f v d\mathbf{x}, \quad \forall\ K \in \mathcal{T}_h. \tag{2.2}$$

The numerical flux $\widehat{u_{\mathbf{n}}}$ which approximates the normal derivative $u_{\mathbf{n}} = \nabla u \cdot \mathbf{n}$ involves the solution jump $[\![u]\!]$, the normal derivative average $\{\{u_{\mathbf{n}}\}\}$ and higher order normal derivative jumps of u on the edge,

$$\widehat{u_{\mathbf{n}}} = \beta_0 \frac{[\![u]\!]}{h_e} + \{\{u_{\mathbf{n}}\}\} + \beta_1 h_e [\![u_{\mathbf{nn}}]\!] + \beta_2 h_e^3 [\![u_{\mathbf{4n}}]\!] + \cdots.$$

In [17], we show it is hard to identify suitable coefficient β_2 to obtain optimal convergence for high order P_k ($k \geq 4$) approximations. Thus we add extra interface terms and have the DDG method with interface correction in [18] such that optimal convergence is obtained for any order approximations. Furthermore, we introduce same format numerical flux for the test function and obtain the symmetric [24] and nonsymmetric version [27] of the DDG methods. Now we summarize scheme formulations of DDG variations for model equation (1.2) as follows,

$$\int_K \nabla u \cdot \nabla v d\mathbf{x} - \int_{\partial K} \widehat{u_{\mathbf{n}}} v ds + \sigma \int_{\partial K} \widetilde{v_{\mathbf{n}}} [\![u]\!] ds = \int_K f v d\mathbf{x}, \quad \text{for all } v \in V_h, \tag{2.3}$$

with $\widehat{u_{\mathbf{n}}}$ and $\widetilde{v_{\mathbf{n}}}$ defined on the interior element edge $\partial K \in \mathcal{E}_h^I$ as,

$$\begin{cases} \widehat{u_{\mathbf{n}}} = \widehat{\nabla u \cdot \mathbf{n}} = \beta_{0u} \frac{[\![u]\!]}{h_e} + \{\{u_{\mathbf{n}}\}\} + \beta_1 h_e [\![u_{\mathbf{nn}}]\!], \\ \widetilde{v_{\mathbf{n}}} = \widetilde{\nabla v \cdot \mathbf{n}} = \beta_{0v} \frac{[\![v]\!]}{h_e} + \{\{v_{\mathbf{n}}\}\} + \beta_1 h_e [\![v_{\mathbf{nn}}]\!]. \end{cases} \tag{2.4}$$

We drop higher order terms and only keep the jump, normal derivative average $\{\{u_{\mathbf{n}}\}\}$ and second order normal derivative jump $[\![u_{\mathbf{nn}}]\!]$ terms in the numerical flux formula. Notice that

the test function $v \in V_h^k$ is taken being zero outside the element K. In a word, only one side contributes to the calculation of $\widetilde{v_{\mathbf{n}}}$ on ∂K. Thus term $\widetilde{v_{\mathbf{n}}}$ essentially degenerates to,

$$\widetilde{v_{\mathbf{n}}} = \left(\beta_{0v}\frac{(-v)}{h_e} + \frac{1}{2}v_{\mathbf{n}} + \beta_1 h_e(-v_{\mathbf{nn}})\right)\Big|_{\partial K}.$$

To apply Dirichlet type boundary condition, i.e. $\partial K \in \mathcal{E}_h^D \subset \partial\Omega$, we have,

$$\widehat{u_{\mathbf{n}}} = \beta_{0u}\frac{[\![u]\!]}{h_e} + u_{\mathbf{n}} \quad \text{with } [\![u]\!] = u_0 - u, \quad \text{and} \quad \widetilde{v_{\mathbf{n}}} = \beta_{0v}\frac{-v}{h_e} + v_{\mathbf{n}}. \tag{2.5}$$

If a Neumann type boundary condition is given, i.e. $u_{\mathbf{n}} = \frac{\partial u}{\partial \mathbf{n}} = g$ is available on $\partial\Omega$, we directly applies

$$\widehat{u_{\mathbf{n}}} = g, \quad \text{on} \quad \partial K \in \partial\Omega.$$

In the numerical flux formula (2.4), h_e is taken as the length of edge $e = K \cap K'$ or the average $h_e = (h_K + h_{K'})/2$ with h_K and $h_{K'}$ being the diameters of element K and K'. Numerically we observe no essential difference with either choice of h_e. The coefficients β_{0u}, β_{0v} and β_1 are chosen to ensure the stability and convergence of these methods. Depending on the sign of $\sigma = +1$ or $\sigma = -1$ in (2.3), correspondingly we have the symmetric and nonsymmetric version of DDG methods. Now we list the three variations of DDG methods and discuss their properties in details.

1. *DDG method with interface correction* [18]:

$$\sigma = +1 \text{ in (2.3) with } \widetilde{v_{\mathbf{n}}} = \{\{v_{\mathbf{n}}\}\} \text{ in (2.4)} \tag{2.6}$$

   with $\beta_1 = 0$ in the numerical flux $\widehat{u_{\mathbf{n}}}$ of (2.4), the DDG method with interface correction [18] degenerates to the symmetric Interior Penalty method. With $\beta_1 \neq 0$, optimal convergence is observed with a small fixed penalty coefficient applied for all P_k polynomial approximations. For example, we choose fixed $\beta_{0u} = 2$ for all P_k ($k \leq 9$) polynomials in [18]. As is well known, the penalty coefficient (β_{0u} in this case) should be taken large enough, roughly in the scale of k^2 for P_k polynomials to stablize the symmetric Interior Penalty method.
2. *Symmetric DDG method* [24]:

$$\sigma = +1 \text{ in (2.3) with (2.4)} \tag{2.7}$$

   In [24], we apply same format numerical flux for the test function and obtain a symmetric DDG scheme. Optimal L^2 error estimate is proved. Analytically we show that any (β_0, β_1) coefficients pair, with $\beta_0 = \beta_{0u} + \beta_{0v}$ in (2.4), that satisfies a quadratic form inequality

$$\beta_0 > 4\left((\beta_1)^2\frac{k^2(k^2-1)^2}{3} - \beta_1\frac{k^2(k^2-1)}{2} + \frac{k^2}{4}\right),$$

   leads to an admissible numerical flux, and guarantees the optimal convergence of the symmetric DDG method.
3. *Nonsymmetric DDG method* [27]:

$$\sigma = -1 \text{ in (2.3) with (2.4)} \tag{2.8}$$

   with $\beta_1 = 0$ in (2.4), the nonsymmetric DDG scheme [27] degenerates to the Baumann and Oden [5] method ($\beta_0 = \beta_{0u} - \beta_{0v} = 0$) or the NIPG [22] method ($\beta_0 = \beta_{0u} - \beta_{0v} > 0$). With $\beta_1 \neq 0$, we observe optimal $(k+1)$th order convergence for any P_k polynomial

approximations, see [27], which improves the sub-optimal kth order convergence of Baumann–Oden and NIPG methods.

Next we consider DDG scheme formulation for the following variable coefficient linear diffusion equation,

$$-\nabla \cdot (K(\mathbf{x})\nabla u) = f.$$

The symmetric DDG scheme formulation for above variable coefficient elliptic equation is to find DG solution $u \in V_h^k$ such that $\forall v \in V_h^k$ and on any element $K \in \mathcal{T}_h$, we have,

$$\int_K K(\mathbf{x})\nabla u \cdot \nabla v \, d\mathbf{x} - \int_{\partial K} \widehat{K(\mathbf{x})\nabla u} \cdot \mathbf{n} v \, ds + \int_{\partial K} \widetilde{K(\mathbf{x})\nabla v} \cdot \mathbf{n}[\![u]\!] \, ds = \int_K f v d\mathbf{x}. \tag{2.9}$$

Here the diffusion coefficient matrix is denoted as $K(\mathbf{x}) = (k_{ij}(\mathbf{x}))$ with $\mathbf{x} \in \Omega$. With normal vector $\mathbf{n} = (n_1, n_2)$ and coefficient $k_{ij}(\mathbf{x})$ well defined on the edge ∂K, the numerical flux can be written out in detail as $\widehat{K(\mathbf{x})\nabla u} \cdot \mathbf{n} = \sum_{i,j=1}^{2} k_{ij}(\mathbf{x}) \widehat{u_{x_j}} n_i$. Similar to (2.4), we have $\widehat{u_{x_j}}$ and $\widetilde{v_{x_j}}$ defined on the edge as follows,

$$\begin{cases} \widehat{u_{x_j}} = \beta_{0u} \frac{[\![u]\!]}{h_e} n_j + \{\{u_{x_j}\}\} + \beta_1 h_e [\![u_{x_j x_1} n_1 + u_{x_j x_2} n_2]\!], \\ \widetilde{v_{x_j}} = \beta_{0v} \frac{[\![v]\!]}{h_e} n_j + \{\{v_{x_j}\}\} + \beta_1 h_e [\![v_{x_j x_1} n_1 + v_{x_j x_2} n_2]\!]. \end{cases}$$

Remark 2.1 For poisson Eq. (1.2), symmetric DDG method is the only one giving symmetric stiffness matrix such that fast solvers can be applied. The rest three DDG methods lead to nonsymmetric linear system.

Remark 2.2 We take Taylor expansion polynomials around element center as basis functions in our numerical tests. To simplify the comparisons among all four DDG methods (2.10), we choose fixed coefficient $\beta_1 = 1/40$ in all examples for P_k $(2 \le k \le 4)$ approximations even there exists a large class of admissible (β_0, β_1) coefficient pair (i.e. symmetric DDG method).

To simplify the discussion and presentation, we focus on Poisson Eq. (1.2) associated with zero Dirichlet boundary condition $u|_{\partial\Omega} = u_0 = 0$ for the following theoretical discussions in this article. We can trivially extend the results to linear Eq. (1.1). Now summing up (2.3) over all elements $K \in \mathcal{T}_h$, we have the primal formulation of DDG method and its variations of (1.2) as: find $u \in V_h^k$ such that

$$B_h(u, v) = F(v), \quad \forall v \in V_h^k. \tag{2.10}$$

The bilinear form $B_h(w, v)$ is listed below as,

$$\begin{aligned} B_h(w, v) := & \sum_{K \in \mathcal{T}_h} \int_K \nabla w \cdot \nabla v d\mathbf{x} + \sum_{e \in \mathcal{E}_h^I} \int_e \left(\widehat{w_{\mathbf{n}}} [\![v]\!] ds + \sigma \widetilde{v_{\mathbf{n}}} [\![w]\!] \right) ds \\ & + \sum_{e \in \mathcal{E}_h^D} \int_e \left(\frac{\beta_0}{h_e} w v - w_{\mathbf{n}} v - \sigma v_{\mathbf{n}} w \right) ds, \end{aligned} \tag{2.11}$$

with the right hand side $F(v)$ given as,

$$F(v) = \int_\Omega f v d\mathbf{x}.$$

Here we have $\beta_0 = \beta_{0u} + \sigma\beta_{0v}$. Again, it degenerates to the original DDG method when taking $\sigma = 0$ in (2.11). Coupled with (2.4) and taking $\sigma = \pm 1$ in (2.11), we have the symmetric and nonsymmetric version of the DDG methods. The DDG with interface correction is the case with $\sigma = +1$ in (2.11) and with test function numerical flux taken as the average $\widetilde{v_{\mathbf{n}}} = \{\{v_{\mathbf{n}}\}\}$.

3 Boundedness, Stability and Error Estimate

In this section, we carry out a unified error estimate for the DDG method and its variations (2.10). We first list approximation properties of the solution space V_h^k and discuss the boundedness and stability of the bilinear form $B_h(\cdot,\cdot)$. Then we establish a suitable energy norm error estimate for the four DDG methods (2.10). Toward the end of this section, we obtain the optimal error estimate under L^2 norm for DDG with interface correction and symmetric DDG methods.

First let's define the energy norm for $v \in V_h^k$:

$$|||v|||_h := \left(\sum_{K\in\mathcal{T}_h} \int_K \nabla v \cdot \nabla v d\mathbf{x} + \sum_{e\in\mathcal{E}_h^I} \int_e \frac{[\![v]\!]^2}{h_e} ds + \sum_{e\in\mathcal{E}_h^D} \int_e \frac{v^2}{h_e} ds \right)^{1/2}. \tag{3.1}$$

3.1 Approximation Properties and Stability

Below we list the trace inequality and inverse inequality of the solution space V_h^k. We refer to finite element textbooks, i.e, [7] or [21] regarding these classical results.

Lemma 3.1 (Trace inequality) *For any element $K \in \mathcal{T}_h$ and $v \in H^s(K)$ with $s \geq 1$, there exist positive constants C_g independent of K such that, $\forall e \subset \partial K$, we have,*

$$\begin{aligned}
&\|v\|_{L^2(e)} \leq C_g h_K^{-1/2} \left(\|v\|_{L^2(K)} + h_K \|\nabla v\|_{\mathbf{L}^2(K)} \right), \\
&\|v_{\mathbf{n}}\|_{L^2(e)} = \|\nabla v \cdot \mathbf{n}\|_{L^2(e)} \leq C_g h_K^{-1/2} \left(\|\nabla v\|_{\mathbf{L}^2(K)} + h_K \|\nabla^2 v\|_{\mathbf{L}^2(K)} \right).
\end{aligned}$$

Lemma 3.2 (Inverse inequality) *For any element $K \in \mathcal{T}_h$ and $v \in P_k(K)$, there exist positive constants C_t, C_i independent of K such that, $\forall\, e \subset \partial K$ and $\forall\, 0 \leq j \leq k$, we have,*

$$\begin{aligned}
&\|v\|_{L^2(e)} \leq C_t h_K^{-1/2} \|v\|_{L^2(K)}, \\
&\|v_{\mathbf{n}}\|_{L^2(e)} = \|\nabla v \cdot \mathbf{n}\|_{L^2(e)} \leq C_t h_K^{-1/2} \|\nabla v\|_{\mathbf{L}^2(K)}, \\
&\|\nabla^j v\|_{\mathbf{L}^2(K)} \leq C_i h_K^{-j} \|v\|_{L^2(K)}.
\end{aligned}$$

Next we establish the continuity and coercivity of the bilinear form (2.11).

Theorem 3.1 *There exist positive constants C_s, C_b for DDG method and its variations (2.10) such that for any $w, v \in V_h^k$, we have,*

$$|B_h(w,v)| \leq C_b |||v|||_h |||w|||_h. \tag{3.2}$$

$$B_h(v,v) \geq C_s |||v|||_h^2, \tag{3.3}$$

Proof Plug in the numerical flux formula (2.4) in (2.11), we have the bilinear form laid out in detail as,

$$B_h(w,v) = \sum_{K\in\mathcal{T}_h}\int_K \nabla w\cdot\nabla v d\mathbf{x} + \sum_{e\in\mathcal{E}_h^I}\int_e \left(\frac{\beta_0}{h_e}[\![w]\!] + \{\{w_{\mathbf{n}}\}\} + \beta_1 h_e [\![w_{\mathbf{nn}}]\!]\right)[\![v]\!] ds$$
$$+\sigma\sum_{e\in\mathcal{E}_h^I}\int_e \left(\{\{v_{\mathbf{n}}\}\} + \beta_1 h_e [\![v_{\mathbf{nn}}]\!]\right)[\![w]\!] ds + \sum_{e\in\mathcal{E}_h^D}\int_e \left(\frac{\beta_0}{h_e} wv - w_{\mathbf{n}} v - \sigma v_{\mathbf{n}} w\right) ds. \tag{3.4}$$

We first show the continuity (3.2) of the bilinear form. We consider $\int_e \{\{w_{\mathbf{n}}\}\}[\![v]\!] ds$ and $\int_e \beta_1 h_e [\![w_{\mathbf{nn}}]\!][\![v]\!] ds$ as example terms and treat other terms in the bilinear form of (3.4) in a similar fashion. Using Cauchy–Schwarz inequality, we have,

$$\int_e \{\{w_{\mathbf{n}}\}\}[\![v]\!] ds \le \|\{\{w_{\mathbf{n}}\}\}\|_{L^2(e)} \left\|[\![v]\!]\right\|_{L^2(e)} \quad \text{and}$$
$$\int_e \beta_1 h_e [\![w_{\mathbf{nn}}]\!][\![v]\!] ds \le \beta_1 h_e \left\|[\![w_{\mathbf{nn}}]\!]\right\|_{L^2(e)} \left\|[\![v]\!]\right\|_{L^2(e)}.$$

Now let's study these two terms in detail. We intensively apply inverse inequalities (Lemma 3.2) to bound the polynomial integral on edge by its integrals over the elements and essentially by its energy norm. Let's assume edge e is a common edge shared by elements K_1 and K_2. With the definition of average $\{\cdot\}$ and jump $[\![\cdot]\!]$, we have,

$$\|\{\{w_{\mathbf{n}}\}\}\|_{L^2(e)} \le \frac{1}{2}\left\|(w_{\mathbf{n}})|_{K_1}\right\|_{L^2(e)} + \frac{1}{2}\left\|(w_{\mathbf{n}})|_{K_2}\right\|_{L^2(e)},$$

and

$$\left\|[\![w_{\mathbf{nn}}]\!]\right\|_{L^2(e)} \le \left\|(w_{\mathbf{nn}})|_{K_1}\right\|_{L^2(e)} + \left\|(w_{\mathbf{nn}})|_{K_2}\right\|_{L^2(e)}.$$

Applying inverse inequalities, we bound the line integral on edge by its integrals over the elements as,

$$\|\{\{w_{\mathbf{n}}\}\}\|_{L^2(e)} \le \frac{C_t}{2} h_{K_1}^{-1/2} \|\nabla w\|_{\mathbf{L}^2(K_1)} + \frac{C_t}{2} h_{K_2}^{-1/2} \|\nabla w\|_{\mathbf{L}^2(K_2)}.$$

Similarly the line integral $\|w_{\mathbf{nn}}|_{K_1}\|_{L^2(e)}$ restricted from the K_1 side can be bounded as,

$$\left\|w_{\mathbf{nn}}|_{K_1}\right\|_{L^2(e)} = \|\nabla w_{\mathbf{n}}\cdot\mathbf{n}\|_{L^2(e)} \le C_t h_{K_1}^{-1/2} \|\nabla w_{\mathbf{n}}\|_{\mathbf{L}^2(K_1)}$$
$$\le C_t C_i h_{K_1}^{-3/2} \|w_{\mathbf{n}}\|_{L^2(K_1)} \le \sqrt{2} C_t C_i h_{K_1}^{-3/2} \|\nabla w\|_{\mathbf{L}^2(K_1)}.$$

Notice that h_K denotes the diameter or the longest edge of element K, thus we have $h_e \le h_{K_1}$ and $h_e \le h_{K_2}$ with $e = \partial K_1 \cap \partial K_2$. Now combine the previous arguments and we obtain,

$$\int_e \{\{w_{\mathbf{n}}\}\}[\![v]\!] ds \le \frac{C_t}{2}\left(h_{K_1}^{-1/2}\|\nabla w\|_{\mathbf{L}^2(K_1)} + h_{K_2}^{-1/2}\|\nabla w\|_{\mathbf{L}^2(K_2)}\right)\left\|[\![v]\!]\right\|_{L^2(e)}$$
$$\le \frac{C_t}{2}\left((h_e/h_{K_1})^{1/2}\|\nabla w\|_{\mathbf{L}^2(K_1)} + \left(h_e/h_{K_2}\right)^{1/2}\|\nabla w\|_{\mathbf{L}^2(K_2)}\right) h_e^{-1/2}\left\|[\![v]\!]\right\|_{L^2(e)}$$
$$\le \frac{C_t}{2}\left(\|\nabla w\|_{\mathbf{L}^2(K_1)} + \|\nabla w\|_{\mathbf{L}^2(K_2)}\right) h_e^{-1/2}\left\|[\![v]\!]\right\|_{L^2(e)},$$

and

$$\begin{aligned}\int_e \beta_1 h_e [\![w_{\mathbf{nn}}]\!][\![v]\!] ds &\le \beta_1 h_e \left\| [\![w_{\mathbf{nn}}]\!] \right\|_{L^2(e)} \left\| [\![v]\!] \right\|_{L^2(e)} \\ &\le \sqrt{2}\beta_1 h_e C_t C_i \left(h_{K_1}^{-3/2} \|\nabla w\|_{\mathbf{L}^2(K_1)} + h_{K_2}^{-3/2} \|\nabla w\|_{\mathbf{L}^2(K_2)} \right) \left\| [\![v]\!] \right\|_{L^2(e)} \\ &\le \sqrt{2}\beta_1 C_t C_i \left(\|\nabla w\|_{\mathbf{L}^2(K_1)} + \|\nabla w\|_{\mathbf{L}^2(K_2)} \right) h_e^{-1/2} \|[\![v]\!]\|_{L^2(e)}.\end{aligned}$$

Sum up the estimates over all interior edges $e \in \mathcal{E}_h^I$ and we have,

$$\begin{aligned}\sum_{e\in\mathcal{E}_h^I} \int_e \{\{w_{\mathbf{n}}\}\}[\![v]\!] ds &\le \frac{C_t}{2} \sum_{e\in\mathcal{E}_h^I} \left(\|\nabla w\|_{\mathbf{L}^2(K_1)} + \|\nabla w\|_{\mathbf{L}^2(K_2)} \right) h_e^{-1/2} \|[\![v]\!]\|_{L^2(e)} \\ &\le \frac{\sqrt{2}}{2} C_t \sum_{e\in\mathcal{E}_h^I} \left(\|\nabla w\|_{\mathbf{L}^2(K_1)}^2 + \|\nabla w\|_{\mathbf{L}^2(K_2)}^2 \right)^{1/2} h_e^{-1/2} \|[\![v]\!]\|_{L^2(e)} \\ &\le \frac{\sqrt{6}}{2} C_t \left(\sum_{K\in\mathcal{T}_h} \|\nabla w\|_{\mathbf{L}^2(K)}^2 \right)^{1/2} \left(\sum_{e\in\mathcal{E}_h^I} h_e^{-1} \|[\![v]\!]\|_{L^2(e)}^2 \right)^{1/2} \\ &\le \frac{\sqrt{6}}{2} C_t |\!|\!| w |\!|\!|_h |\!|\!| v |\!|\!|_h, \end{aligned} \tag{3.5}$$

and

$$\begin{aligned}\sum_{e\in\mathcal{E}_h^I} \int_e \beta_1 h_e [\![w_{\mathbf{nn}}]\!][\![v]\!] ds &\le \sqrt{2} C_t C_i \beta_1 \sum_{e\in\mathcal{E}_h^I} \left(\|\nabla w\|_{\mathbf{L}^2(K_1)} + \|\nabla w\|_{\mathbf{L}^2(K_2)} \right) h_e^{-1/2} \|[\![v]\!]\|_{L^2(e)} \\ &\le 2\beta_1 C_t C_i \sum_{e\in\mathcal{E}_h^I} \left(\|\nabla w\|_{\mathbf{L}^2(K_1)}^2 + \|\nabla w\|_{\mathbf{L}^2(K_2)}^2 \right)^{1/2} h_e^{-1/2} \|[\![v]\!]\|_{L^2(e)} \\ &\le 2\sqrt{3}\beta_1 C_t C_i \left(\sum_{K\in\mathcal{T}_h} \|\nabla w\|_{\mathbf{L}^2(K)}^2 \right)^{1/2} \left(\sum_{e\in\mathcal{E}_h^I} h_e^{-1} \|[\![v]\!]\|_{L^2(e)}^2 \right)^{1/2} \\ &\le 2\sqrt{3}\beta_1 C_t C_i |\!|\!| w |\!|\!|_h |\!|\!| v |\!|\!|_h. \end{aligned} \tag{3.6}$$

For edges falling on domain boundary, we use similar method to bound the terms and we have,

$$\begin{aligned}\sum_{e\in\mathcal{E}_h^D} \int_e (-w_{\mathbf{n}} v)\, ds &\le C_t \left(\sum_{\substack{K\in\mathcal{T}_h \\ \partial K\cap\partial\Omega\neq\emptyset}} \|\nabla w\|_{\mathbf{L}^2(K)}^2 \right)^{1/2} \left(\sum_{e\in\mathcal{E}_h^D} h_e^{-1} \|[\![v]\!]\|_{L^2(e)}^2 \right)^{1/2} \\ &\le C_t |\!|\!| w |\!|\!|_h |\!|\!| v |\!|\!|_h. \end{aligned}$$

Back to the bilinear form $B_h(w, v)$ of (3.4), we apply estimates (3.5)–(3.6) to the example terms and treat other terms in the bilinear form similarly and finally we have,

$$
\begin{aligned}
|B_h(w,v)| \le & \sum_{K\in\mathcal{T}_h} \|\nabla w\|_{\mathbf{L}^2(K)}\|\nabla v\|_{\mathbf{L}^2(K)} + \sum_{e\in\mathcal{E}_h} \beta_0 h_e^{-1}\|[\![w]\!]\|_{L^2(e)}\|[\![v]\!]\|_{L^2(e)} \\
& + \frac{\sqrt{6}}{2}C_t|\!|\!|w|\!|\!|_h|\!|\!|v|\!|\!|_h + 2\sqrt{3}\beta_1 C_t C_i|\!|\!|w|\!|\!|_h|\!|\!|v|\!|\!|_h + \frac{\sqrt{6}}{2}C_t|\!|\!|v|\!|\!|_h|\!|\!|w|\!|\!|_h \\
& + 2\sqrt{3}\beta_1 C_t C_i|\!|\!|v|\!|\!|_h|\!|\!|w|\!|\!|_h + 2C_t|\!|\!|w|\!|\!|_h|\!|\!|v|\!|\!|_h \\
\le & \, C_b|\!|\!|w|\!|\!|_h|\!|\!|v|\!|\!|_h,
\end{aligned}
$$

where $C_b = 1 + \beta_0 + 4\sqrt{3}\beta_1 C_t C_i + \left(\sqrt{6}+2\right)C_t$. We are finished with the continuity discussion of (3.2).

To obtain the coercivity of the bilinear form (3.3), again we consider example terms (3.5)–(3.6) and we apply Young's inequality. For any $\delta > 0$ and $\varepsilon > 0$, we have,

$$
\sum_{e\in\mathcal{E}_h^I}\int_e \{\{w_{\mathbf{n}}\}\}[\![v]\!]ds \le \frac{1}{2\varepsilon}\sum_{K\in\mathcal{T}_h}\|\nabla w\|^2_{\mathbf{L}^2(K)} + \frac{3}{4}\varepsilon C_t^2\sum_{e\in\mathcal{E}_h^I} h_e^{-1}\|[\![v]\!]\|^2_{L^2(e)},
$$

and

$$
\sum_{e\in\mathcal{E}_h^I}\int_e \beta_1 h_e[\![w_{\mathbf{nn}}]\!][\![v]\!]ds \le \frac{1}{2\delta}\sum_{K\in\mathcal{T}_h}\|\nabla w\|^2_{\mathbf{L}^2(K)} + 6\delta\beta_1^2 C_t^2 C_i^2\sum_{e\in\mathcal{E}_h^I} h_e^{-1}\|[\![v]\!]\|^2_{L^2(e)}.
$$

Handle other terms in the bilinear form similarly and we have,

$$
\begin{aligned}
B_h(v,v) \ge & \left(1 - \frac{1}{\varepsilon} - \frac{1}{\delta}\right)\sum_{K\in\mathcal{T}_h}\|\nabla v\|^2_{\mathbf{L}^2(K)} \\
& + \sum_{e\in\mathcal{E}_h}\left(\beta_0 - 12\delta\beta_1^2 C_t^2 C_i^2 - \frac{5}{2}\varepsilon C_t^2\right)h_e^{-1}\|[\![v]\!]\|^2_{L^2(e)}.
\end{aligned}
$$

We can choose ε, δ and β_0 such that $1 - \frac{1}{\varepsilon} - \frac{1}{\delta} > 0$ and $\beta_0 > 12\delta\beta_1^2 C_t^2 C_i^2 + \frac{5}{2}\varepsilon C_t^2$. Now take $C_S = \min\{1 - \frac{1}{\varepsilon} - \frac{1}{\delta}, \beta_0 - 12\delta\beta_1^2 C_t^2 C_i^2 - \frac{5}{2}\varepsilon C_t^2\}$ and we obtain the stability of the bilinear form (3.3). □

3.2 Energy Norm and L^2 Norm Error Estimates

According to Theorem 3.1, it is easy to obtain the following theorem.

Theorem 3.2 *There exists a unique solution $u \in V_h^k$ for problem (2.10).*

Proof Since (2.10) is a linear problem in finite dimensional space, existence is equivalent to uniqueness. We assume that there are two numerical solutions u^1 and u^2. Then we have the difference $w = u^1 - u^2$ satisfying

$$
B_h(w,w) = 0.
$$

By the coercivity result (3.3), we have $|\!|\!|w|\!|\!|_h = 0$ which directly implies that $u^1 = u^2$. □

Theorem 3.3 *Let $u_{ex} \in H^{k+1}(\Omega)\cap C^2(\Omega)$ be the exact solution of Poisson Eq. (1.2) with zero Dirichlet boundary and we have $u \in V_h^k$ denote one of the four DDG schemes (2.10) solutions, we have,*

$$
B_h(u_{ex} - u, v) = 0, \quad \forall v \in V_h^k. \tag{3.7}
$$

Proof We denote by u_{ex} the exact solution, thus we have (2.1) holding true for any $v \in V_h^k$. Summing (2.1) over all elements $K \in \mathcal{T}_h$ and formally we have,

$$\sum_{K\in\mathcal{T}_h}\int_K \nabla u_{ex}\cdot\nabla v d\mathbf{x} - \sum_{K\in\mathcal{T}_h}\int_{\partial K}\nabla u_{ex}\cdot\mathbf{n} v ds = \int_\Omega f v d\mathbf{x}.$$

With $u_{ex} \in C^2(\Omega)$, we have $[\![u_{ex}]\!] = 0$, $\{\{\nabla u_{ex}\cdot\mathbf{n}\}\} = \nabla u_{ex}\cdot\mathbf{n}$ and $[\![(u_{ex})_{\mathbf{nn}}]\!] = 0$ across over any interelement edge ∂K. We also have $u_{ex}|_{\partial\Omega} = 0$ with the zero Dirichlet boundary condition. With boundary condition (2.5) applied, the definition of numerical flux (2.4) and the bilinear form (2.11), for any $v \in \mathbb{V}_h^k$, we have the exact solution satisfying the bilinear form as below,

$$\begin{aligned} B_h(u_{ex}, v) = &\sum_{K\in\mathcal{T}_h}\int_K \nabla u_{ex}\cdot\nabla v d\mathbf{x} + \sum_{e\in\mathcal{E}_h^I}\int_e \widehat{\nabla u_{ex}\cdot\mathbf{n}}[\![v]\!] + \sigma\widetilde{v_{\mathbf{n}}}[\![u_{ex}]\!] ds \\ &+ \sum_{e\in\mathcal{E}_h^D}\int_e\left(\frac{\beta_0}{h_e}u_{ex}v - \nabla u_{ex}\cdot\mathbf{n}v - \sigma v_{\mathbf{n}}u_{ex}\right)ds = \int_\Omega f v d\mathbf{x} = F(v). \end{aligned}$$

This directly implies that (3.7) holds true. □

Theorem 3.4 *Let $u_{ex} \in H^{k+1}(\Omega)\cap C^2(\Omega)$ be the exact solution of (1.2) with zero Dirichlet boundary and $u \in V_h^k$ be one of the four DDG schemes (2.10) solutions, then we have,*

$$|\!|\!| u_{ex} - u |\!|\!|_h \le C h^k |u_{ex}|_{H^{k+1}(\Omega)}. \tag{3.8}$$

Proof Let $Iu_{ex} \in V_h^k$ denote the continuous interpolation polynomial of u_{ex} over the element edges, then we have standard approximation error as,

$$\forall\, 0 \le s \le k+1, \quad |u_{ex} - Iu_{ex}|_{H^s(K)} \le C_I h_K^{k+1-s}|u_{ex}|_{H^{k+1}(K)}, \quad \forall K \in \mathcal{T}_h. \tag{3.9}$$

Since both u_{ex} and Iu_{ex} are continuous thus we have zero jumps $[\![u_{ex} - Iu_{ex}]\!] = 0$ across interelement edges. From (3.1) and with zero Dirichlet boundary condition applied we have,

$$|\!|\!| u_{ex} - Iu_{ex} |\!|\!|_h = \sum_{K\in\mathcal{T}_h}\int_K \nabla(u_{ex} - Iu_{ex})\cdot\nabla(u_{ex} - Iu_{ex}) d\mathbf{x} \le C_I h^k |u_{ex}|_{H^{k+1}(\Omega)}. \tag{3.10}$$

Coupled with above interpolation error (3.10), we see the estimate of $|\!|\!| u_{ex} - u |\!|\!|_h$ can be easily obtained once we have estimate on $|\!|\!| u - Iu_{ex} |\!|\!|_h$. For convenience, let's denote the error between DDG numerical solution and exact solution interpolation as $\chi = u - Iu_{ex}$. We have u and $Iu_{ex} \in V_h^k$ and $[\![u_{ex} - Iu_{ex}]\!] = 0$ across interelement edges. With Theorem 3.1 and Theorem 3.3 we have,

$$\begin{aligned} C_s |\!|\!| u - Iu_{ex} |\!|\!|_h^2 &\le B_h(u - Iu_{ex}, \chi) = B_h(u - u_{ex} + u_{ex} - Iu_{ex}, \chi) \\ &= B_h(u_{ex} - Iu_{ex}, \chi) \\ &= \sum_{K\in\mathcal{T}_h}\int_K \nabla(u_{ex} - Iu_{ex})\cdot\nabla\chi d\mathbf{x} \\ &\quad + \sum_{e\in\mathcal{E}_h^I}\int_e \left(\{\{\nabla(u_{ex} - Iu_{ex})\cdot\mathbf{n}\}\} + \beta_1 h_e [\![(u_{ex} - Iu_{ex})_{\mathbf{nn}}]\!]\right)[\![\chi]\!] ds \\ &\quad - \sum_{e\in\mathcal{E}_h^D}\int_e \nabla(u_{ex} - Iu_{ex})\cdot\mathbf{n}\chi\, ds. \end{aligned} \tag{3.11}$$

To obtain the estimate on $|||u - Iu_{ex}|||_h$, we need to further estimate the right hand side terms of the above equality (3.11). Using Cauchy–Schwarz inequality, we obtain bounds on the last three items as,

$$\sum_{e\in\mathcal{E}_h^I}\int_e \{\{\nabla(u_{ex}-Iu_{ex})\cdot\mathbf{n}\}\}[\![\chi]\!]ds \le \sum_{e\in\mathcal{E}_h^I} h_e^{1/2}\,\|\{\{\nabla(u_{ex}-Iu_{ex})\cdot\mathbf{n}\}\}\|_{L^2(e)}\, h_e^{-1/2}\,\|[\![\chi]\!]\|_{L^2(e)},$$

$$\sum_{e\in\mathcal{E}_h^I}\int_e \beta_1 h_e[\![(u_{ex}-Iu_{ex})_{\mathbf{nn}}]\!][\![\chi]\!]ds \le \sum_{e\in\mathcal{E}_h^I} \beta_1 h_e\,\|[\![(u_{ex}-Iu_{ex})_{\mathbf{nn}}]\!]\|_{L^2(e)}\,\|[\![\chi]\!]\|_{L^2(e)},$$

and

$$\sum_{e\in\mathcal{E}_h^D}\int_e \nabla(u_{ex}-Iu_{ex})\cdot\mathbf{n}\chi ds \le \sum_{e\in\mathcal{E}_h^D} h_e^{1/2}\,\|\nabla(u_{ex}-Iu_{ex})\cdot\mathbf{n}\|_{L^2(e)}\, h_e^{-1/2}\|\chi\|_{L^2(e)}.$$

Again we assume edge e is a generic interior edge shared by elements K_1 and K_2, thus we have,

$$\begin{aligned}\|\{\{\nabla(u_{ex}-Iu_{ex})\}\}\cdot\mathbf{n}\|_{L^2(e)} \le{}& \frac{1}{2}\left\|\nabla(u_{ex}-Iu_{ex})\cdot\mathbf{n}|_{K_1}\right\|_{L^2(e)}\\ &+\frac{1}{2}\left\|\nabla(u_{ex}-Iu_{ex})\cdot\mathbf{n}|_{K_2}\right\|_{L^2(e)},\end{aligned}$$

and

$$\left\|[\![(u_{ex}-Iu_{ex})_{\mathbf{nn}}]\!]\right\|_{L^2(e)} \le \left\|(u_{ex}-Iu_{ex})_{\mathbf{nn}}|_{K_1}\right\|_{L^2(e)} + \left\|(u_{ex}-Iu_{ex})_{\mathbf{nn}}|_{K_2}\right\|_{L^2(e)}.$$

Furthermore, with trace inequality of Lemma 3.1 and interpolation error (3.9) we have,

$$\begin{aligned}\left\|\nabla(u_{ex}-Iu_{ex})\cdot\mathbf{n}|_{K_1}\right\|_{L^2(e)} &\le C_g h_{K_1}^{-1/2}\big(h\|\nabla(u_{ex}-Iu_{ex})\|_{\mathbf{L}^2(K_1)}\\ &\quad + h_{K_1}\|\nabla^2(u_{ex}-Iu_{ex})\|_{\mathbf{L}^2(K_1)}\big)\\ &\le 6C_gC_I h_{K_1}^{k-1/2}|u_{ex}|_{H^{k+1}(K_1)},\end{aligned}$$

and

$$\begin{aligned}\left\|(u_{ex}-Iu_{ex})_{\mathbf{nn}}|_{K_1}\right\|_{L^2(e)} &\le C_g h_{K_1}^{-1/2}\big(\|(u_{ex}-Iu_{ex})_{\mathbf{nn}}\|_{L^2(K_1)}\\ &\quad + h_{K_1}\|\nabla(u_{ex}-Iu_{ex})_{\mathbf{nn}}\|_{\mathbf{L}^2(K_1)}\big)\\ &\le 3C_gC_I h_{K_1}^{k-3/2}|u_{ex}|_{H^{k+1}(K_1)}.\end{aligned}$$

Collect all estimates of the right hand side terms of (3.11) and we have,

$$C_s|||\chi|||_h^2 \le (9C_g + 9C_g\beta_1 + 1)C_I h^k|u_{ex}|_{H^{k+1}(\Omega)}|||\chi|||_h,$$

or

$$|||u - Iu_{ex}|||_h \le Ch^k|u_{ex}|_{H^{k+1}(\Omega)}.$$

Applying triangle inequality and with (3.10), we directly obtain,

$$|||u_{ex}-u|||_h \le |||u_{ex}-Iu_{ex}|||_h + |||Iu_{ex}-u|||_h \le Ch^k|u_{ex}|_{H^{k+1}(\Omega)}.$$

□

To carry out the error estimate under L^2 norm, we follow standard duality argument. For convenience, we consider continuous linear finite element space $\tilde{V}_h := \{v \in H^1(\Omega) : v|_K \in P_1(K), \forall K \in \mathcal{T}_h, v|_{\partial\Omega} = 0\}$ to solve the auxiliary problem.

Theorem 3.5 *Let $u_{ex} \in H^{k+1}(\Omega) \cap C^2(\Omega)$ solve the boundary value problem (1.2) with zero Dirichlet boundary and we have u denote the DDG method with interface correction (2.6) or symmetric DDG method (2.7) solution of problem (2.10), we have,*

$$\|u_{ex} - u\|_{L^2(\Omega)} \leq Ch^{k+1} \|u_{ex}\|_{H^{k+1}(\Omega)}. \tag{3.12}$$

Proof We start with the following auxiliary problem:

$$-\Delta\psi = u_{ex} - u, \text{ on } \Omega, \quad \text{with Dirichlet boundary } \psi|_{\partial\Omega} = 0. \tag{3.13}$$

Standard regularity result gives,

$$\|\psi\|_{H^2(\Omega)} \leq C\|u_{ex} - u\|_{L^2(\Omega)}. \tag{3.14}$$

We solve auxiliary problem (3.13) and denote $\psi_h \in \tilde{V}_h$ as the solution of conforming finite element method,

$$\int_\Omega \nabla\psi_h \cdot \nabla v_h d\mathbf{x} = \int_\Omega (u_{ex} - u) v_h d\mathbf{x}, \quad \text{for all } v_h \in \tilde{V}_h. \tag{3.15}$$

Recall that we have following error estimate with linear polynomial approximations,

$$|\psi - \psi_h|_{H^1(\Omega)} \leq Ch|\psi|_{H^2(\Omega)}. \tag{3.16}$$

With regularity result (3.14) we have $\psi \in H^2(\Omega)$, thus we have $\{\{\psi\}\} = \psi$, $[\![\psi]\!] = 0$, $\{\{\nabla\psi \cdot \mathbf{n}\}\} = \nabla\psi \cdot \mathbf{n}$ and $[\![\nabla\psi \cdot \mathbf{n}]\!] = 0$ across interelement edges. Multiply (3.13) with $(u_{ex} - u)$ and integrate over the domain, have integrating by parts over each element and formally we obtain,

$$\begin{aligned}
\|u_{ex} - u\|^2_{L^2(\Omega)} &= -\int_\Omega \Delta\psi(u_{ex} - u)d\mathbf{x} \\
&= \sum_{K\in\mathcal{T}_h} \left(\int_K \nabla\psi \cdot \nabla(u_{ex} - u)d\mathbf{x} - \int_{\partial K} \nabla\psi \cdot \mathbf{n}(u_{ex} - u)ds \right) \\
&= \sum_{K\in\mathcal{T}_h} \int_K \nabla\psi \cdot \nabla(u_{ex} - u)d\mathbf{x} + \sum_{e\in\mathcal{E}_h^I} \int_e \{\{\nabla\psi \cdot \mathbf{n}\}\}[\![u_{ex} - u]\!]ds \\
&\quad - \sum_{e\in\mathcal{E}_h^D} \int_e \nabla\psi \cdot \mathbf{n}(u_{ex} - u)ds.
\end{aligned} \tag{3.17}$$

Notice the numerical solution $[\![u]\!] \neq 0$ over ∂K even the exact solution is continuous across interelement edges. Now we have u denoting the DDGIC (2.6) or symmetric DDG (2.7) solution with bilinear form (2.11). And we have u_{ex} as the exact solution of (1.2) and we have Theorem 3.3 holding true. With $\psi_h \in \tilde{V}_h$ as the continuous linear finite element solution of (3.15), we have $[\![\psi_h]\!] = 0$ and $[\![(\psi_h)_{\mathbf{nn}}]\!] = 0$ across interelement edges. Thus we have,

$$\begin{aligned}
0 = B_h(u_{ex} - u, \psi_h) &= \sum_{K\in\mathcal{T}_h} \int_K \nabla(u_{ex} - u) \cdot \nabla\psi_h d\mathbf{x} + \sum_{e\in\mathcal{E}_h^I} \int_e \{\{\nabla\psi_h \cdot \mathbf{n}\}\}[\![u_{ex} - u]\!]ds \\
&\quad - \sum_{e\in\mathcal{E}_h^D} \int_e \nabla\psi_h \cdot \mathbf{n}(u_{ex} - u)ds.
\end{aligned}$$

Finally we subtract the right hand side of (3.17) from above equality, combine the results of (3.16) and (3.14) and apply Cauchy–Schwarz inequality as in Theorem 3.4, we have,

$$\begin{aligned}\|u_{ex}-u\|^2_{L^2(\Omega)} &= \sum_{K\in\mathcal{T}_h}\int_K \nabla(\psi-\psi_h)\cdot\nabla(u_{ex}-u)d\mathbf{x}\\ &\quad+\sum_{e\in\mathcal{E}_h^I}\int_e \{\{\nabla(\psi-\psi_h)\cdot\mathbf{n}\}\}[\![u_{ex}-u]\!]ds\\ &\quad-\sum_{e\in\mathcal{E}_h^D}\int_e \nabla(\psi-\psi_h)\cdot\mathbf{n}(u_{ex}-u)ds\\ &\le Ch|\psi|_{H^2(\Omega)}|\!|\!|u_{ex}-u|\!|\!|_h \le Ch\|u_{ex}-u\|_{L^2(\Omega)}|\!|\!|u_{ex}-u|\!|\!|_h.\end{aligned}$$

Applying the energy norm error estimates (3.8), we complete the proof. □

4 Numerical Examples

In this section we provide a sequence of numerical examples to illustrate the accuracy and capability of DDG method and its variations (2.10). For the linear system, we use a restarted GMRES method solving a nonsymmetric system and conjugate gradient method solving the symmetric ones. To obtain machine level precision, we set the stopping criterion as the relative residual norm less than 10^{-12}. Notice that for most problems presented in this section we have analytical or exact solution available such that the right hand side function f can be calculated from the available function. Dirichlet boundary condition is given with the exact solution's restriction on the domain boundary.

We use following notations to denote the errors between exact solution and numerical solution:

$$\|e_h\|_{L^\infty}:=\|u_{ex}-u\|_{L^\infty(\Omega)},\quad \|e_h\|_{L^2}:=\|u_{ex}-u\|_{L^2(\Omega)},\quad |\!|\!|e_h|\!|\!|_h:=|\!|\!|u_{ex}-u|\!|\!|_h.$$

Furthermore, we have e_h and $e_{h/2}$ representing the error at two consecutive triangulations with mesh size h and $h/2$, respectively. The order is calculated with,

$$\text{order}=\frac{1}{\ln(2)}\ln\left(\frac{\|e_h\|}{\|e_{h/2}\|}\right),$$

where $\|\cdot\|$ represents the L^∞ norm, the L^2 norm or the energy norm (3.1).

Example 4.1 Convex domain with structured and unstructured triangular meshes.

We start with the accuracy check of the four DDG methods (2.10) on Poisson Eq. (1.2) on convex domain $\Omega=[0,1]\times[0,1]$. Right hand side function is given with

$$f(x_1,x_2)=4\left(1-x_1^2-x_2^2\right)exp\left(-x_1^2-x_2^2\right).$$

Exact solution is available with $u_{ex}=exp\left(-x_1^2-x_2^2\right)$. We consider implementations of the four DDG methods on three different meshes: structured uniform mesh and nonuniform mesh (Fig. 1) and unstructured mesh (Fig. 2).

The structured nonuniform mesh is setup by dividing a uniform mesh interval into three sub-intervals in each axis direction. More precisely, let's denote a uniform mesh with $\tilde{x}_i=ih$

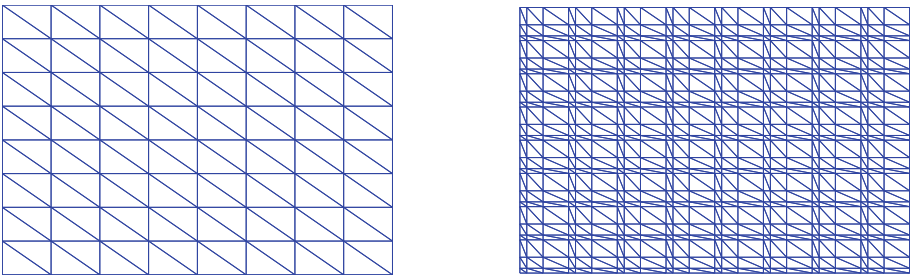

Fig. 1 Uniform mesh (*left*) and nonuniform mesh (*right*)

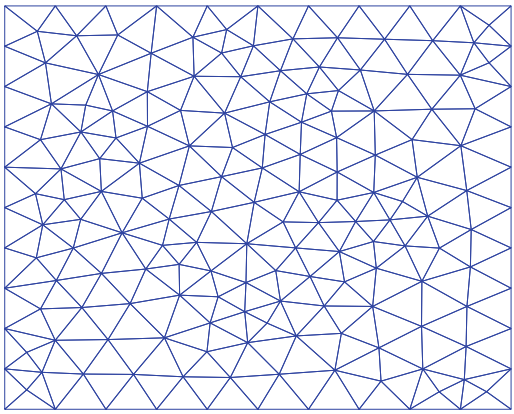

Fig. 2 Unstructured mesh with 312 *triangles*

for $i = 0, \ldots, M$, where $h = 1/M$ and $\tilde{x}_M = 1$. The nonuniform mesh nodes are generated and denoted as follows,

$$\begin{aligned} x_{3i} &= \tilde{x}_i, \\ x_{3i+1} &= x_{3i} + \gamma_1 h, \\ x_{3i+2} &= x_{3i+1} + \gamma_2 h. \end{aligned}$$

Here γ_1 and γ_2 are positive numbers with $\gamma_1 + \gamma_2 < 1$.

On uniform mesh, DDG method (2.2) loses order with even order P_2 polynomial approximations. This is similar to the DDG method for time dependent problem [17] in which it shows it is hard to identify suitable coefficient β_1 to obtain optimal convergence. For DDGIC (2.6) and symmetric (2.7) and nonsymmetric (2.8) DDG methods, optimal $(k+1)$th order convergence is obtained under both L^2 and L^∞ norms. To save space, we only list the error table for symmetric DDG method, see Table 1.

For implementations on the dramatic nonuniform mesh (right one in Fig. 1), we observe order loss for DDG method (2.2) and nonsymmetric DDG method (2.8) with even order polynomial approximations, see Table 2 for nonsymmetric DDG method. Notice that NIPG method obtains sub-optimal order convergence for all P_k polynomial approximations, see [15] on nonuniform mesh accuracy check. Both DDGIC and symmetric DDG methods obtain $(k+1)$th optimal order convergence on nonuniform mesh, see Table 3 for DDGIC and Table 4 for symmetric DDG method. Accuracy check on unstructured mesh (Fig. 2) is carried out also and similar results are obtained. To save space, again we only list the accuracy table for symmetric DDG method, see Table 5.

Table 1 Symmetric DDG method (2.7) on uniform mesh

k, β_0, β_1	h	$\|e_h\|_{L^\infty}$	Order	$\|e_h\|_{L^2}$	Order	$\|\|e_h\|\|_h$	Order
2	0.0441	2.9436e−6		3.3292e−7		1.2203e−4	
$\beta_0 = 4.5$	0.0221	3.7064e−7	2.99	4.1431e−8	3.01	3.0299e−5	2.01
$\beta_1 = 1/40$	0.0111	4.6493e−8	2.99	5.1683e−9	3.00	7.5483e−6	2.01
3	0.0883	4.2937e−7		3.8198e−8		9.1896e−6	
$\beta_0 = 10$	0.0441	2.7352e−8	3.97	2.4180e−9	3.98	1.1260e−6	3.03
$\beta_1 = 1/40$	0.0221	1.7177e−9	3.99	1.5205e−10	3.99	1.3934e−7	3.01
4	0.0883	5.9843e−9		7.0176e−10		6.8940e−8	
$\beta_0 = 17.5$	0.0441	1.8814e−10	4.99	2.2270e−11	4.98	4.2068e−9	4.03
$\beta_1 = 1/40$	0.0221	5.9658e−12	4.98	7.0296e−13	4.98	2.5808e−10	4.03

Table 2 Nonsymmetric DDG (2.8) on nonuniform mesh with $\gamma_1 = 1/7, \gamma_2 = 1/3$

k, β_0, β_1	h	$\|e_h\|_{L^\infty}$	Order	$\|e_h\|_{L^2}$	Order	$\|\|e_h\|\|_h$	Order
2	0.1767	2.4247e−5		7.7742e−6		3.7785e−4	
$\beta_0 = 9$	0.0883	4.6354e−6	2.39	1.7602e−6	2.14	9.4698e−5	2.00
$\beta_1 = 1/40$	0.0441	1.0069e−6	2.20	4.2384e−7	2.05	2.3701e−5	2.00
3	0.1767	3.1900e−7		3.7846e−8		6.8443e−6	
$\beta_0 = 20$	0.0883	2.0142e−8	3.99	2.4086e−9	3.97	8.6424e−7	2.99
$\beta_1 = 1/40$	0.0441	1.2723e−9	3.98	1.5403e−10	3.97	1.0857e−7	2.99

Table 3 DDGIC (2.6) on nonuniform mesh with $\gamma_1 = 1/7, \gamma_2 = 1/3$

k, β_0, β_1	h	$\|e_h\|_{L^\infty}$	Order	$\|e_h\|_{L^2}$	Order	$\|\|e_h\|\|_h$	Order
2	0.1767	2.5595e−5		3.1923e−6		7.4743e−4	
$\beta_0 = 9$	0.0883	3.4943e−6	2.87	4.1920e−7	2.93	2.0669e−4	1.85
$\beta_1 = 1/40$	0.0441	4.4934e−7	2.96	5.3843e−8	2.96	5.4425e−5	1.93
3	0.1767	2.7517e−7		3.2693e−8		7.2357e−6	
$\beta_0 = 20$	0.0883	1.7467e−8	3.98	2.0766e−9	3.98	9.1033e−7	2.99
$\beta_1 = 1/40$	0.0441	1.0958e−9	3.99	1.3113e−10	3.99	1.1413e−7	3.00

Table 4 Symmetric DDG (2.7) on nonuniform mesh with $\gamma_1 = 1/7, \gamma_2 = 1/3$

k, β_0, β_1	h	$\|e_h\|_{L^\infty}$	Order	$\|e_h\|_{L^2}$	Order	$\|\|e_h\|\|_h$	Order
2	0.1767	8.3208e−5		6.3453e−6		1.5841e−3	
$\beta_0 = 9$	0.0883	1.0209e−5	3.03	8.0069e−7	2.99	3.9949e−4	1.99
$\beta_1 = 1/40$	0.0441	1.2655e−6	3.01	1.0048e−7	2.99	1.0024e−4	1.99
3	0.1767	2.8447e−7		3.2200e−8		7.0980e−6	
$\beta_0 = 10$	0.0883	1.8050e−8	3.99	2.0449e−9	3.98	8.9171e−7	2.99
$\beta_1 = 1/40$	0.0441	1.1325e−9	3.99	1.2891e−10	3.99	1.1172e−7	3.00

Table 5 Symmetric DDG (2.7) on unstructured mesh with 312, 1248 and 4992 triangle elements

k, β_0, β_1	h	$\|e_h\|_{L^\infty}$	Order	$\|e_h\|_{L^2}$	Order	$\|\|\|e_h\|\|\|_h$	Order
2	0.1040	3.7275e−5		7.7305e−6		7.7561e−4	
$\beta_0 = 9$	0.0520	4.6531e−6	3.19	9.7652e−7	2.98	1.9526e−4	1.99
$\beta_1 = 1/40$	0.0260	5.7993e−7	3.42	1.2274e−7	2.99	4.9014e−5	1.99
3	0.1040	1.3490e−6		9.5439e−8		1.7929e−5	
$\beta_0 = 10$	0.0520	9.1784e−8	3.88	5.8792e−9	4.02	2.0540e−6	3.13
$\beta_1 = 1/40$	0.0260	5.5303e−9	4.05	3.6396e−10	4.01	2.4350e−7	3.08

Table 6 CPU time comparison between symmetric DDG and SIPG methods

	h	$k = 3$	$k = 4$
Symmetric DDG	0.0883	1.0936e+1	9.0262e+1
$\beta_0 = 9$	0.0441	2.4983e+1	4.8143e+2
$\beta_1 = 1/40$	0.0221	9.8452e+1	1.6275e+3
SIPG	0.0883	1.0015e+1	8.6636e+1
$\beta_0 = 9$	0.0441	2.8033e+1	3.6640e+2
	0.0221	1.0500e+2	1.7717e+3

We also consider efficiency issues of the DDG methods. Among the four DDG methods, symmetric DDG method (2.7) is the most suitable elliptic solver. The linear system of symmetric DDG method has symmetric structure and is easy to apply fast solvers. We calculate the mass matrix condition numbers of DDGIC and symmetric DDG methods, which are on the order of $O(h^{-1.97})$. When comparing with SIPG method, symmetric DDG method gains roughly 7–10 % on CPU time for high order approximations, see Table 6.

Example 4.2 Accuracy check on L-shaped domain.

In this example, we solve Laplace equation on the L-shaped nonconvex domain $\Omega = [-1, 1] \times [-1, 1] \backslash ([0, 1] \times [-1, 0]$. Dirichlet boundary condition is applied. Exact solution is available (in polar coordinates) with $u_{ex}(r, \theta) = r^{2/3} \left(\sin\left(\frac{2}{3}\theta\right) + \cos\left(\frac{2}{3}\theta\right)\right)$. Notice that the regularity of the solution is that $u_{ex} \in H^{\frac{5}{3}-\epsilon}$ for any $\epsilon > 0$. The partial derivatives of the solution are singular at the origin.

We use uniform mesh (Fig. 3) to carry out convergence studies for the DDG method and its variations (2.10). For all four schemes, we obtain close to $\frac{5}{3}$th order convergence under L^2 norm. In Table 7 we list the errors and orders of nonsymmetric DDG method (2.8). Slightly better convergence is observed with DDGIC and symmetric DDG methods, see Table 8 for symmetric DDG method.

Example 4.3 Interface problem with discontinuous diffusion coefficients.

We solve the following variable coefficient elliptic problem,

$$-\nabla(K(\mathbf{x})\nabla u) = f(\mathbf{x}), \quad \mathbf{x} \in \Omega = [0, 1] \times [0, 1],$$

with Dirichlet boundary condition. The diffusion coefficient matrix $K(\mathbf{x})$ is diagonal $K(\mathbf{x}) = diag(k)$ with $k = \{10, 10^{-1}, 10^3, 1\}$ that is piecewise defined in four subregions, see Fig. 4

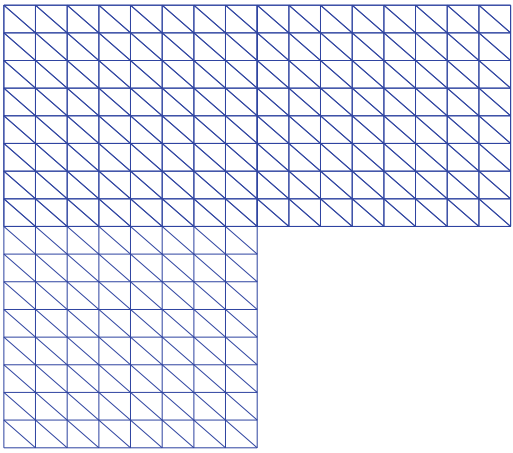

Fig. 3 Uniform mesh on L-shaped domain

Table 7 L-shaped domain with nonsymmetric DDG method (2.8), uniform mesh

k, β_0, β_1	h	$\|e_h\|_{L^\infty}$	Order	$\|e_h\|_{L^2}$	Order	$\|\|e_h\|\|_h$	Order
2	0.0883	2.7717e−2		3.1753e−4		3.1585e−2	
$\beta_0 = 9$	0.0441	1.7463e−2	0.67	1.2407e−4	1.36	1.9898e−2	0.67
$\beta_1 = 1/40$	0.0221	1.1001e−2	0.67	4.8731e−5	1.35	1.2535e−2	0.67
3	0.1767	2.6474e−2		3.8978e−4		2.6189e−2	
$\beta_0 = 20$	0.0883	1.6679e−2	0.67	1.4724e−4	1.40	1.6499e−2	0.67
$\beta_1 = 1/40$	0.0441	1.0508e−2	0.67	5.6427e−5	1.38	1.0393e−2	0.67

Table 8 L-shaped domain with symmetric DDG method (2.7), uniform mesh

k, β_0, β_1	h	$\|e_h\|_{L^\infty}$	Order	$\|e_h\|_{L^2}$	Order	$\|\|e_h\|\|_h$	Order
2	0.0441	1.9342e−2		6.7832e−5		2.1932e−2	
$\beta_0 = 4.5$	0.0221	1.2185e−2	0.67	2.4089e−5	1.49	1.3816e−2	0.67
$\beta_1 = 1/40$	0.0111	7.6760e−3	0.67	8.7786e−6	1.46	8.7037e−3	0.67
3	0.0883	1.8182e−2		5.2013e−5		1.7658e−2	
$\beta_0 = 10$	0.0441	1.1454e−2	0.67	1.7115e−5	1.60	1.1124e−2	0.67
$\beta_1 = 1/40$	0.0221	7.2157e−3	0.67	5.7378e−6	1.58	7.0077e−3	0.67

(also in [14]). Correspondingly the two interface lines are $x_1 = x_c = 0.5$ and $x_2 = y_c = 0.5$. Uniform triangular mesh partitioned along interface lines is considered. Exact solution is available with,

$$u_{ex} = \frac{1}{k} \sin\left(\frac{\pi x_1}{2}\right)(x_1 - x_c)(x_2 - y_c)\left(1 + x_1^2 + x_2^2\right).$$

The solution itself is continuous but the gradient is discontinuous across interfaces lines. For the given interface jump conditions $[\![u]\!] = 0$ and $[\![-K(\mathbf{x})\nabla u \cdot \mathbf{n}]\!] = 0$, we make no modification on our scheme formulations to explicitly enforce the jump conditions. With

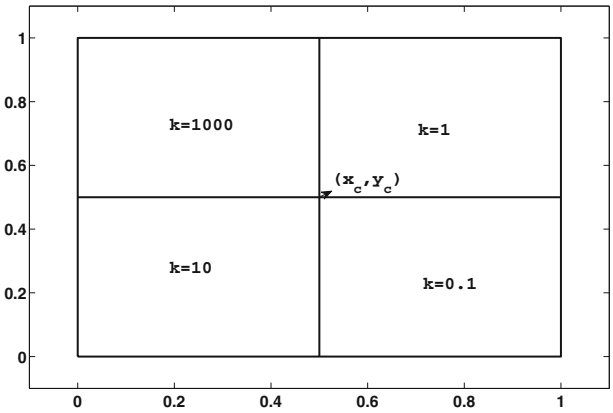

Fig. 4 Piecewise constant diffusion coefficients $k = \{10, 10^{-1}, 10^3, 1\}$

Table 9 Interface problem with DDGIC method

k, β_0, β_1	h	$\|e_h\|_{L^\infty}$	Order	$\|e_h\|_{L^2}$	Order	$\|\|\|e_h\|\|\|_h$	Order
2	0.0883	4.4576e−4		2.9017e−5		5.5796e−3	
$\beta_0 = 9$	0.0441	5.6738e−5	2.97	3.6032e−6	3.01	1.3841e−3	2.01
$\beta_1 = 1/40$	0.0221	7.1481e−6	2.99	4.4852e−7	3.01	3.4439e−4	2.01
3	0.1767	1.4570e−4		6.0110e−6		8.2941e−4	
$\beta_0 = 20$	0.0883	1.0756e−5	3.76	3.9296e−7	3.94	9.8683e−5	3.07
$\beta_1 = 1/40$	0.0441	7.5058e−7	3.84	2.5112e−8	3.97	1.1792e−5	3.07

zero flux jump across the interface, we see the flux $K(\mathbf{x})\nabla u \cdot \mathbf{n}$ itself is continuous and well defined on the interface lines. For element edge ∂K that falls on the interface, we incorporate the discontinuous diffusion coefficients $K(\mathbf{x})$ into the numerical flux $\widehat{K(\mathbf{x})\nabla u} \cdot \mathbf{n}$ definition. For example, suppose the element edge ∂K falls on interface line $x_2 = y_c = 0.5$ with outward normal $\mathbf{n} = (0, 1)$, the numerical flux degenerates to $\widehat{K(\mathbf{x})\nabla u} \cdot \mathbf{n} = \widehat{(ku)_{x_2}}$ and we have,

$$\widehat{ku_{x_2}} = \beta_0 \frac{k^+u^+ - k^-u^-}{h_e} + \frac{k^-u^-_{x_2} + k^+u^+_{x_2}}{2} + \beta_1 h_e \left(k^+u^+_{x_2x_2} - k^-u^-_{x_2x_2}\right).$$

Here we have diffusion coefficient $k = k^+$ for $x_2 > 0.5$ and $k = k^-$ for $x_2 < 0.5$ and u^+ and u^- correspondingly denote the value of u on edge ∂K evaluated from its neighbor element and from its own element. Thus the zero flux interface jump condition is applied WEAKLY in our implementations.

We carry out P_2 and P_3 polynomial approximations and list the errors and orders in Tables 9 and 10 for DDGIC and symmetric DDG methods. We obtain $(k + 1)$th order convergence under both L^2 and L^∞ norms. Solution simulations with P_2 polynomials and mesh size $h = 0.0441$ are shown in Fig. 5.

Example 4.4 Peak solution.

In this example, we solve Poisson equation with a peak solution. The domain is set as $\Omega = [0, 1]\times[0, 1]$ and Dirichlet boundary condition is applied. The exact solution is available with expression,

Table 10 Interface problem with Symmetric DDG method

k, β_0, β_1	h	$\|e_h\|_{L^\infty}$	Order	$\|e_h\|_{L^2}$	Order	$\|\|\|e_h\|\|\|_h$	Order
2	0.0883	4.5410e−4		2.8896e−5		5.5306e−3	
$\beta_0 = 4.5$	0.0441	5.7782e−5	2.97	3.5862e−6	3.01	1.3716e−3	2.01
$\beta_1 = 1/40$	0.0221	7.2784e−6	2.99	4.4619e−7	3.01	3.4122e−4	2.01
3	0.1767	1.4534e−4		6.0525e−6		8.3195e−4	
$\beta_0 = 10$	0.0883	1.0669e−5	3.77	3.9484e−7	3.94	9.8893e−5	3.07
$\beta_1 = 1/40$	0.0441	7.4418e−7	3.84	2.5218e−8	3.97	1.1816e−5	3.07

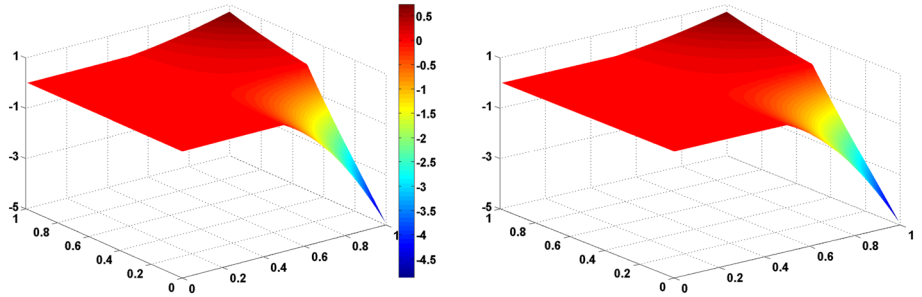

Fig. 5 Interface problem with DDGIC (*left*) and symmetric DDG (*right*) methods

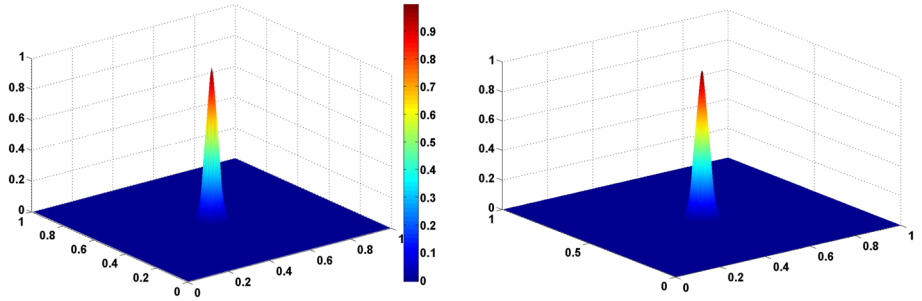

Fig. 6 Peak solution simulations by DDGIC (*left*) and symmetric DDG (*right*) methods

$$u_{ex} = exp\left(-\alpha\left((x_1 - x_c)^2 + (x_2 - y_c)^2\right)\right),$$

where $(x_c, y_c) = (0.5, 0, 5)$ is the location of the peak and $\alpha = 1000$ determines the strength of the peak. Approximations with DDGIC (2.6) and symmetric DDG (2.7) methods are carried out and shown in Fig. 6 with uniform triangulation mesh $h = 0.0441$ and P_2 polynomial approximations. The sharp peak is resolved very well with these two schemes.

Example 4.5 Highly oscillatory wave solution for Helmholtz equation.

In this example we solve Helmholtz equation with variable coefficients as follows,

$$-\Delta u - \frac{1}{(\alpha + r)^4} u = f, \quad \text{with} \quad r = \sqrt{(x_1)^2 + (x_2)^2}.$$

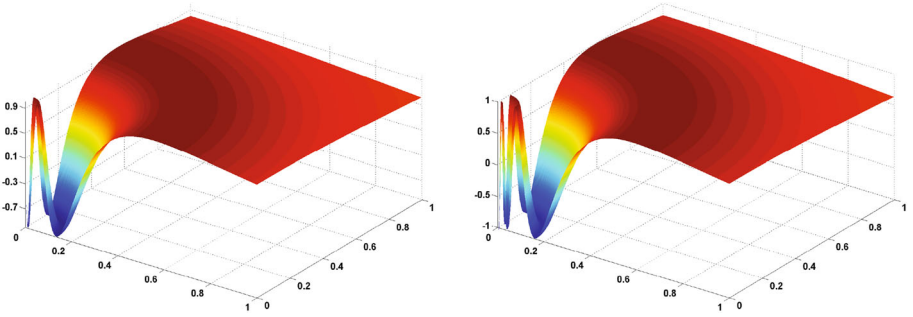

Fig. 7 Oscillatory solution by DDGIC (*left*) and symmetric DDG (*right*) methods

The square domain is set as $\Omega = [0, 1] \times [0, 1]$ and Dirichlet boundary condition is applied. We have $\alpha = \frac{1}{N\pi}$ where the integer N determines the number of oscillatory waves near the origin. Exact solution is given with $u_{ex} = \sin\left(\frac{1}{\alpha+r}\right)$.

We apply uniform triangular mesh with $h = 0.0110$ and quadratic P_2 approximations in this example. The number of oscillations is taken with $N = 4$ in α. The solution is supposed to be highly oscillatory near the origin. As shown in Fig. 7, with same mesh and polynomial approximations applied, symmetric DDG method (2.7) resolves the highly oscillatory wave better than the DDGIC method (2.6).

Acknowledgments Huang's work is supported by Natural Science Foundation of Zhejiang Province Grant Nos. LY14A010002 and LY12A01009, and is subsidized by the National Natural Science Foundation of China under Grant Nos. 11101368, 11471195, 11001168 and 11202187. Yan's research is supported by the US National Science Foundation (NSF) under grant DMS-1620335.

References

1. Arnold, D.N.: An interior penalty finite element method with discontinuous elements. SIAM J. Numer. Anal. **19**(4), 742–760 (1982)
2. Arnold, D.N., Brezzi, F., Cockburn, B., Marini, L.D.: Unified analysis of discontinuous Galerkin methods for elliptic problems. SIAM J. Numer. Anal. **39**(5), 1749–1779 (2002). (electronic)
3. Baker, G.A.: Finite element methods for elliptic equations using nonconforming elements. Math. Comput. **31**, 45–59 (1977)
4. Bassi, F., Rebay, S.: A high-order accurate discontinuous finite element method for the numerical solution of the compressible Navier–Stokes equations. J. Comput. Phys. **131**(2), 267–279 (1997)
5. Baumann, C.E., Oden, J.T.: A discontinuous *hp* finite element method for convection-diffusion problems. Comput. Methods Appl. Mech. Eng. **175**(3–4), 311–341 (1999)
6. Brenner, S.C., Owens, L., Sung, L.-Y.: A weakly over-penalized symmetric interior penalty method. Electron. Trans. Numer. Anal. **30**, 107–127 (2008)
7. Brenner, S.C., Scott, L.R.: The Mathematical Theory of Finite Element Methods, Volume 15 of Texts in Applied Mathematics, 3rd edn. Springer, New York (2008)
8. Brezzi, F., Douglas Jr., J., Marini, L.D.: Two families of mixed finite elements for second order elliptic problems. Numer. Math. **47**(2), 217–235 (1985)
9. Cockburn, B., Gopalakrishnan, J., Lazarov, R.: Unified hybridization of discontinuous Galerkin, mixed, and continuous Galerkin methods for second order elliptic problems. SIAM J. Numer. Anal. **47**(2), 1319–1365 (2009)
10. Cockburn, B., Johnson, C., Shu, C.-W., Tadmor, E.: Advanced numerical approximation of nonlinear hyperbolic equations, volume 1697 of Lecture Notes in Mathematics. In: Quarteroni, A. (ed.) Papers from the C.I.M.E. Summer School Held in Cetraro, 23–28 June 1997. Springer-Verlag, Berlin (1998). Fondazione C.I.M.E. [C.I.M.E. Foundation]

11. Cockburn, B., Shu, C.-W.: The local discontinuous Galerkin method for time-dependent convection-diffusion systems. SIAM J. Numer. Anal. **35**(6), 2440–2463 (1998). (electronic)
12. Cockburn, B., Shu, C.-W.: Runge–Kutta discontinuous Galerkin methods for convection-dominated problems. J. Sci. Comput. **16**(3), 173–261 (2001)
13. Di Pietro, D.A., Ern, A.: Mathematical Aspects of Discontinuous Galerkin Methods, Volume 69 of Mathématiques & Applications (Berlin) [Mathematics & Applications]. Springer, Heidelberg (2012)
14. Ewing, R., Iliev, O., Lazarov, R.: A modified finite volume approximation of second-order elliptic equations with discontinuous coefficients. SIAM J. Sci. Comput. **23**(4), 1335–1351 (2001)
15. Guzmán, J., Rivière, B.: Sub-optimal convergence of non-symmetric discontinuous Galerkin methods for odd polynomial approximations. J. Sci. Comput. **40**(1–3), 273–280 (2009)
16. Hesthaven, J.S., Warburton, T.: Nodal Discontinuous Galerkin Methods, Volume 54 of Texts in Applied Mathematics. Springer, New York (2008). (Algorithms, analysis, and applications)
17. Liu, H., Yan, J.: The direct discontinuous Galerkin (DDG) methods for diffusion problems. SIAM J. Numer. Anal. **47**(1), 475–698 (2009)
18. Liu, H., Yan, J.: The direct discontinuous Galerkin (DDG) method for diffusion with interface corrections. Commun. Comput. Phys. **8**(3), 541–564 (2010)
19. Oden, J.T., Babuška, I., Baumann, C.E.: A discontinuous *hp* finite element method for diffusion problems. J. Comput. Phys. **146**(2), 491–519 (1998)
20. Raviart, P.-A., Thomas, J.M.: A mixed finite element method for 2nd order elliptic problems. In: Mathematical Aspects of Finite Element Methods (Proc. Conf., Consiglio Naz. delle Ricerche (C.N.R.), Rome, 1975). Lecture Notes in Math., Vol. 606, pp. 292–315. Springer, Berlin (1977)
21. Rivière, B.: Discontinuous Galerkin Methods for Solving Elliptic and Parabolic Equations Volume 35 of Frontiers in Applied Mathematics. Society for Industrial and Applied Mathematics (SIAM), Philadelphia (2008). (Theory and implementation)
22. Rivière, B., Wheeler, M.F., Girault, V.: A priori error estimates for finite element methods based on discontinuous approximation spaces for elliptic problems. SIAM J. Numer. Anal. **39**(3), 902–931 (2001). (electronic)
23. Shu, C-w: Discontinuous Galerkin method for time-dependent problems: survey and recent developments. In: Recent developments in discontinuous Galerkin finite element methods for partial differential equations, volume 157 of IMA Vol. Math. Appl., pp. 25–62. Springer, Cham (2014)
24. Vidden, C., Yan, J.: A new direct discontinuous Galerkin method with symmetric structure for nonlinear diffusion equations. J. Comput. Math. **31**(6), 638–662 (2013)
25. Wang, J., Ye, X.: A weak Galerkin finite element method for second-order elliptic problems. J. Comput. Appl. Math. **241**, 103–115 (2013)
26. Wheeler, M.F.: An elliptic collocation-finite element method with interior penalties. SIAM J. Numer. Anal. **15**, 152–161 (1978)
27. Yan, J.: A new nonsymmetric discontinuous Galerkin method for time dependent convection diffusion equations. J. Sci. Comput. **54**(2–3), 663–683 (2013)